MECSOL 2019 - Proceedings of the 7th International Symposium on Solid Mechanics
V. Tita, A. Ferreira, M.L. Ribeiro, A. Vieira and A.T. Beck (Editors), ABCM, Sao Carlos, SP, Brazil, April 15th to 17th, 2019

A Thermodynamically Consistent Phase Field Framework for Anisotropic Structural Damage

Ana Luísa Evaristo Rocha Petrini[1], Marco Lucio Bittencourt[1] and José Luis Boldrini [1]

[1] Department of Integrated Systems, School of Mechanical Engineering, University of Campinas, SP, 13083-970, Brazil

Abstract. Many phase field formulations have been developed to simulate damage evolution taking into account different phenomena such as plasticity, large deformation, anisotropy and fracture behavior of materials. In the present work, a thermodynamic consistent damage phase field formulation is adapted to include the anisotropic effect of preferential cleavage planes in the damage evolution. A phase field damage scalar variable is associated with each predefined preferential direction of crack propagation. Any other possible different direction is penalized by a parameter ($\beta >> 1$) that represents the degree of anisotropy of the fracture. By defining $\beta = 0$, the isotropic case is recovered. In case of more than one preferential direction, the material is considered totally fractured when one of the damage variables reaches one. Preliminary tests show that the model can reproduce the expected crack propagation pattern.
Keywords: Phase field models, Damage, Anisotropy, Finite element method

Introduction

The phase field methodology was originally developed to solve separation of fluids (Cahn, 1959). It has gained large attention as an efficient method to model material damage, specially for avoiding the sharp interface models for cracks. The crack geometry is approximated by a smeared representation defined by a scalar variable φ that depends on the position $\mathbf{x}$ in the body Ω and represents the volumetric fraction of damaged material. For virgin material, $\varphi = 0$, for fractured material $\varphi = 1$ and $0 < \varphi < 1$ represents damaged material between these two states. Accurate crack propagation patterns for different materials have been obtained (Miehe et al., 2010; Borden et al., 2012).

Describing initiation of damage, its evolution and ultimately the fracture for different types of materials with consistent mathematical models is one of the major difficulties nowadays (Boldrini et al., 2016). A general thermodynamically consistent non-isothermal continuum thermo-mechanic framework for the evolution of damage, fatigue and fracture in materials under the hypothesis of small deformation can be found in Boldrini et al. (2016). Their approach is based on the use of the principle of virtual power (PVP), the balance of energy and the Clausius–Duhem inequality for the entropy. The damage phase field is described by a continuous dynamic variable. This framework is general and allows the use of different free-energy potentials for many types of materials (Boldrini et al., 2016). In the present work, this approach was adapted in order to include an anisotropic damage evolution in a similar manner as described by (Clayton and Knap, 2015; Nguyen et al., 2017). The ideas presented by these authors were chosen due to the easiness of implementation and ability to capture the crack path dependency on the material symmetry, as observed in polycrystalline material or in some additive manufactured materials. However, their models have drawbacks. For example, the manner the damage equation couples with the equation of movement does not make it clear the thermodynamic consistency; furthermore just isothermal cases are considered. Different methods for modeling anisotropic damage and other applications can be found in (Teichtmeister and Miehe, 2015; Mozaffari and Voyiadjis, 2015).
This paper presents a phase field model for a linear elastic brittle material with anisotropic damage evolution. In the first section, the governing equations and the finite element discretization are presented followed by the algorithm used to solve the problem. Finally, the numerical results and conclusions are addressed.

Phase field model for anisotropic crack propagation

The anisotropy in the present model is provided by the existence of preferential cleavage planes as can be observed, for example, in polycrytalline materials. Therefore, preferential directions $\mathbf{m}_i$ $(i = 1,2,...,\mathrm{N})$ for the crack growth are defined and a damage scalar variable φ_i is associated for each preferential direction. The variable $\underline{\varphi}$ and $\nabla\underline{\varphi}$ will represent the dependency of all damage scalar variables and their gradients. Consequently, instead of having only one equation for the damage evolution, there will be N equations of damage phase field, one for each preferential direction. As in the isotropic case developed by (Boldrini et al., 2016), these equations and the coupled equations to solve the displacement $\mathbf{u}$ are obtained by applying the principle of virtual power and the entropy inequality based on a suitable specific free energy

potential (Ψ) that guarantees the thermodynamic consistency.

Considering an incompressible homogeneous material under small strain with material density $\rho = \rho_0$, we have the following system of governing equations for the isothermal case:

$$\begin{cases} \dot{\rho} = 0 & (1a) \\ \rho_0 \ddot{\mathbf{u}} = \text{div}\mathbf{T} + \rho\mathbf{f} \quad \text{in } \Omega & (1b) \\ \tilde{\lambda}_i \, \dot{\varphi}_i = \text{div}\,(\rho_0 \dfrac{\partial \Psi}{\partial \nabla \varphi_i}) - \rho_0 \dfrac{\partial \Psi}{\partial \varphi_i} \quad \text{for } i = 1,2,...,\text{N} & (1c) \\ \mathbf{T} = \rho_0 \dfrac{\partial \Psi}{\partial \mathbf{E}} - \rho_0 \,\text{sym}\,(\sum_{k=1}^{N} \nabla\varphi_k \otimes \dfrac{\partial \Psi}{\partial \nabla \varphi_k}) + \tilde{b}\,\mathbf{D}. & (1d) \end{cases}$$

where $\mathbf{T}$ is the Cauchy stress tensor, $\mathbf{f}$ the body force vector field per unit of mass, $\mathbf{E} = \nabla^s \mathbf{u}$ and $\mathbf{D} = \nabla^s \dot{\mathbf{u}}$. The coefficient $\tilde{b}$ refers to the viscous damping of the material and $\tilde{\lambda}_k$ is associated to the rate of damage change.

By using suitable free-energy functional Ψ in the previous system, it is possible to obtain thermodynamically consistent fracture and fatigue models for many types of materials. To include the possibility of damage, we take the expression of the free-energy density as the sum of the elastic energy density of the cracked body, $\mathcal{E}(\underline{\varphi}, \mathbf{E})$, and the energy density required to create the crack, $\mathcal{J}(\underline{\varphi}, \nabla\underline{\varphi}, \omega)$, according to the Griffith criterion as

$$\rho_0 \psi(\mathbf{E}, \underline{\varphi}, \nabla\underline{\varphi}, \omega) = \mathcal{E}(\underline{\varphi}, \mathbf{E}) + \mathcal{J}(\underline{\varphi}, \nabla\underline{\varphi}, \omega). \tag{2}$$

The elastic energy density of the cracked body is given by:

$$\mathcal{E}(\underline{\varphi}, \mathbf{E}) = \frac{1}{2}\left[\mathbf{E} : \mathbb{C} : \mathbf{E}\right], \tag{3}$$

where $\mathbb{C}$ denote the degraded elastic tensor of the isotropic material:

$$\mathbb{C}(\underline{\varphi}) = g(\underline{\varphi})\mathbb{C}^0 + k_0 \mathbf{1} \otimes \mathbf{1} \left[1 - g(\underline{\varphi})\right] \text{sign}^{-}\text{tr}(\mathbf{E}). \tag{4}$$

$\mathbb{C}^0$ is the elasticity tensor, k_0 is the bulk modulus for the undamaged material and $sign^-(x) = 1$ if $x < 0$ and $sign^-(x) = 0$ if $x \geq 0$. The degradation function $g(\underline{\varphi})$ is commonly taken as a quadratic function, e.g (Miehe et al., 2010; Nguyen et al., 2017). Albeit such form may not be appropriated for the anisotropic case with more than one preferential direction of cleavage, in order to make comparisons of models, the present work has adopted the same $g(\varphi_i)$ as Nguyen et. al (2017):

$$g(\underline{\varphi}) = (1 - \kappa)\prod_{i}^{N}(1 - \varphi_i)^2 + \kappa, \tag{5}$$

$\kappa << 1$ is a small parameter used to maintain the well-posedness of the system in case the damage reaches the unit value.

The second term of the free-energy density (Eq. 2) is based on the concept of crack density function per unit volume γ and the Griffith fracture energy g_c as follows:

$$\mathcal{J}(\underline{\varphi}, \nabla\underline{\varphi}, \omega) = g_c \sum_{k=1}^{N} \gamma_k(\varphi_k, \nabla_k \varphi_k). \tag{6}$$

For the isotropic case, the crack density function γ is defined as

$$\gamma(\varphi, \nabla\varphi) = \frac{1}{2l}\varphi^2 + \frac{l}{2}\nabla\varphi \cdot \nabla\varphi. \tag{7}$$

As adopted by Nguyen et al. (2017), this formulation was extended to the anisotropic case, using the following expressions:

$$\gamma_i(\varphi_i, \nabla\varphi_i) = \frac{1}{2l}{\varphi_i}^2 + \frac{l}{2}\boldsymbol{\omega_i} : (\nabla\varphi_i \otimes \nabla\varphi_i), \tag{8}$$

$$\boldsymbol{\omega_i} = \mathbf{1} + \beta(\mathbf{1} - \mathbf{m}_i \otimes \mathbf{m}_i), \tag{9}$$

where $l > 0$ is a parameter related to the width of the damage phase field layers and ω is the second order structural tensor defined by the unit vector $\mathbf{m}$ normal to the preferential cleavage plane with respect to the material coordinates (Clayton and Knap, 2015). Parameter β is used to control how strong is the tendency of the crack to follow one specific direction. High values of β ($>> 1$) avoid the crack to propagate on planes not normal to $\mathbf{m}$. To recover the isotropic case only one equation of damage must be solved for $\beta = 0$.

Substituting the defined free-energy potential in Eq. 1, the strong formulation reduces to

$$\begin{cases} \ddot{\mathbf{u}} = \dfrac{1}{\rho_0}\mathrm{div}\,(\mathbb{C}:\mathbf{E}) - \dfrac{l g_c}{\rho_0}\mathrm{sym}\displaystyle\sum_{k=1}^{n}\mathrm{div}\,((\omega_k\nabla\varphi_k)\otimes\nabla\varphi_k) + \dfrac{\tilde{b}}{\rho_0}\mathrm{div}\mathbf{D} + \mathbf{f}, & \text{(10a)} \\ \dot{\varphi}_i = \dfrac{g_c l}{\tilde{\lambda}_i}\,\omega_{\mathbf{i}}:\nabla^2\varphi_i + \dfrac{1}{\tilde{\lambda}_i}\mathcal{H}_i - \dfrac{g_c}{\tilde{\lambda}_i\, l}\varphi_i, \qquad \text{for} \quad i = 1,2,...,\mathrm{N} & \text{(10b)} \end{cases}$$

where $\mathcal{H}_k$ is defined as

$$\mathcal{H}_i(x,t) = \max\{(1-\kappa)\textstyle\prod_{k\neq i}(1-\varphi_k)^2\,\mathbf{E}:\mathbb{C}_h:\mathbf{E}\}, \quad \text{with } \mathbb{C}_h = \mathbb{C}^0 - k_0\mathbf{1}\otimes\mathbf{1}\mathrm{sign}^{-}\mathrm{tr}(\mathbf{E}). \tag{11}$$

Finite Element Approximation

In order to solve the problem using the finite element method, each expression in Eq. 10b is multiplied by suitable test functions $\hat{u}$ and $\hat{\varphi}$, and integrated over the domain Ω of the body. After some calculations and application of the boundary conditions (**B.T.**), we obtain the following weak form:

$$\begin{cases} \displaystyle\int_\Omega \ddot{\mathbf{u}}\hat{u}\,d\Omega = -\int_\Omega \frac{1}{\rho_0}\mathbb{C}:\mathbf{E}:\nabla\hat{u}\,d\Omega + \int_\Omega \frac{l g_c}{\rho_0}\,\mathrm{sym}\left(\sum_{k=1}^{n}(\omega_k\nabla\varphi_k)\otimes\nabla\varphi_i\right):\nabla\hat{u}\,d\Omega - \int_\Omega \frac{\tilde{b}}{\rho_0}\,D:\nabla\hat{u}\,d\Omega + \int_\Omega \mathbf{f}\cdot\hat{u}\,d\Omega + \mathbf{B}.\mathbf{T}. & \text{(12a)} \\ \displaystyle\int_\Omega \dot{\varphi}_i\hat{\varphi}\,d\Omega = -\int_\Omega \frac{g_c l}{\tilde{\lambda}_i}(\omega_i\nabla\varphi_i)\cdot\nabla\hat{\varphi}\,d\Omega + \int_\Omega \frac{1}{\tilde{\lambda}_i}\mathcal{H}_i\hat{\varphi}\,d\Omega - \int_\Omega \frac{g_c}{\tilde{\lambda}_i l}\varphi_i\hat{\varphi}\,d\Omega \qquad \text{for } i = 1,2,...,N & \text{(12b)} \end{cases}$$

For the aproximation of the solution, a bidimensional spatial discretization was considered; for details see (Chiarelli et al., 2017). With respect to the time discretization, a semi-implicit scheme is adopted where each equation is solved separately by an implicit method. Firstly, the damage evolution equation for each preferential direction i is solved using the backward Euler method. After that, the damage solutions $\varphi_{i_{n+1}}$ is replaced in the equation of motion which is solved by the standard Newmark method. This procedure is repeated for each time step t_n in the time interval [0, T] with time increments $\Delta t = t_{n+1} - t_n > 0$ for $n = 0, 1, \ldots$.

The time-marching rule for the damage equation related to the preferential direction i at time step $n+1$ is given by

$$\left[\mathbb{M}_\varphi + \Delta t\,(\mathbb{P}_\varphi{}^{n+1} + \mathbb{K}_c{}^{n+1})\right]\varphi_i{}^{n+1} = \mathbb{M}_\varphi\varphi_i{}^{n} + \Delta t\,\mathbf{w}_b{}^{n+1}, \tag{13}$$

with operators obtained by the standard assembling procedure of the element matrices

$$\mathbb{M}_\varphi^{elem} = \int_{\Omega_{elem}} \tilde{\lambda}_k\,\mathbf{N}_\varphi{}^T\mathbf{N}_\varphi\,d\Omega,$$

$$\mathbb{P}_\varphi^{elem} = \int_{\Omega_{elem}} g_c l\mathbf{B}_\varphi{}^T\left(\omega_i\mathbf{B}_\varphi\right)\,d\Omega + \int_{\Omega_{elem}} \frac{g_c}{l}\mathbf{N}_\varphi{}^T\mathbf{N}_\varphi\,d\Omega,$$

$$\mathbb{K}_c^{elem} = \int_{\Omega_{elem}} \hat{\mathcal{H}}_k(\varphi_n,\hat{u}_n^e)\,\mathbf{N}_\varphi{}^T\mathbf{N}_\varphi\,d\Omega,$$

$$\mathbf{w_b}{}^{elem} = \int_{\Omega_{elem}} \hat{\mathcal{H}}_k(\varphi_n,\hat{u}_n^e)\,\mathbf{N}_\varphi{}^T\,d\Omega.$$

The approximate solution of the displacement at time step $n+1$, $\mathbf{u}_{n+1}$, can be computed by solving:

$$[\alpha_1\mathbb{M} + \mathbb{K}_u + \alpha_4\mathbb{K}_v]\,\mathbf{u}^{n+1} = \mathbb{M}\,[\alpha_1\mathbf{u}^n + \alpha_2\dot{\mathbf{u}}^n + \alpha_3\ddot{\mathbf{u}}^n] + \mathbf{w_a} + \mathbb{K}_v\,[\alpha_4\mathbf{u}^n - \alpha_5\dot{\mathbf{u}}^n - \alpha_6\ddot{\mathbf{u}}^n] + \mathbb{M}\mathbf{f}^{n+1}, \tag{14}$$

with operators obtained by the standard assembling procedure of the element matrices

$$\mathbb{M}^{elem} = \int_{\Omega_{elem}} \rho_0\,\mathbf{N}_u{}^T\mathbf{N}_u\,d\Omega,$$

$$\mathbb{K}_u^{elem} = \int_{\Omega_{elem}} \mathbf{B}_u{}^T:\mathbb{C}(\mathbf{N}_\varphi\hat{\varphi}^e):\mathbf{B}_u\,d\Omega,$$

$$\mathbf{w_a}^{elem} = \int_{\Omega_{elem}} g_c l \, \mathbf{B}_u{}^T \text{sym} \left(\sum_{k=1}^{n} \left[(\omega_k \mathbf{B}_\varphi \hat{\varphi}^{e^n}_k) \otimes \mathbf{B}_\varphi \hat{\varphi}^{e^n}_k \right] \right) d\Omega,$$

$$\mathbb{K}_v^{elem} = \int_{\Omega_{elem}} \tilde{b} \, \mathbf{B}_u{}^T \mathbf{B}_u \, d\Omega.$$

After solving the evolution equation for displacement (Eq. 14), the acceleration and velocity fields are updated:

$$\ddot{\mathbf{u}}^{n+1} = \alpha_1(\mathbf{u}^{n+1} - \mathbf{u}^n) - \alpha_2 \dot{\mathbf{u}}^n - \alpha_3 \ddot{\mathbf{u}}^n, \quad (15)$$

$$\dot{\mathbf{u}}^{n+1} = \alpha_4(\mathbf{u}^{n+1} - \mathbf{u}^n) + \alpha_5 \dot{\mathbf{u}}^n + \alpha_6 \ddot{\mathbf{u}}^n. \quad (16)$$

where the coefficients α_j (j = 1,...,6) are given in terms of the Newmark coefficients $\tilde{\gamma} = 0.5$ and $\tilde{\beta} = 0.25$:

$\alpha_1 = \frac{1}{\tilde{\beta}\Delta t^2}$, $\alpha_2 = \frac{1}{\tilde{\beta}\Delta t}$, $\alpha_3 = \frac{1-2\tilde{\beta}}{2\tilde{\beta}}$, $\alpha_4 = \frac{\tilde{\gamma}}{\tilde{\beta}\Delta t}$, $\alpha_5 = 1 - \frac{\tilde{\gamma}}{\tilde{\beta}}$, $\alpha_6 = [1 - \frac{\tilde{\gamma}}{2\tilde{\beta}}]\Delta t$.

The overall procedure is given in Algorithm 1.

Algorithm 1 Time integration for the system of equations

1: **for** $t = 0 \rightarrow T$ **do**
2: Given u_n, $\dot{u}_n$, φ_n and $\tilde{\lambda}_n$, solve equation Eq. (13) for $\varphi_{i_{n+1}}$ with $i = 1$;
3: **if** number of preferential directions $\neq 1$ **then**
4: **for** i = 2:N **do**
5: Given u_n, $\dot{u}_n$, φ_n and $\tilde{\lambda}_n$ and $\varphi_{i-1_{n+1}}$, solve equation Eq. (13) for $\varphi_{i_{n+1}}$;
6: Given the updated damage φ_{n+1}, solve equation Eq. (14) for u_{n+1};
7: From the current displacement u_{n+1}, update the acceleration $\ddot{u}_{n+1}$ and velocity $\dot{u}_{n+1}$ using Eq. (15) and Eq. (16);
8: Update the time step by adding the time increment Δt.

Numerical Results

To verify the ability of the model to reproduce the anisotropic damage, a simulation of an I-shaped tensile test specimen was performed. An isotropic ($\beta = 0$) and an anisotropic material ($\beta = 10$) with preferential direction oriented at -45^o with respect to the horizontal axis were considered. The bottom edge of the specimen is fixed and a vertical prescribed displacement of $1 \times 10^{-4} tm/s$ is applied to the upper edge incrementally through the time steps. In this simulation, we used a mesh of quadratic triangles with 4961 nodes. An initial damage, simulating a pre-crack at 0^0, was set at the nodes as illustrated in Fig. 1(a). The parameters for this case are Young modulus $E = 160\,GPa$, Poisson coefficient $\nu = 0.3$, $\rho_0 = 7300\,kg/m^3$, $g_c = 2.7 \times 10^3\,Nm$ and $l = 2.5 \times 10^{-3}$ as used by Chiarelli et. al (2017).

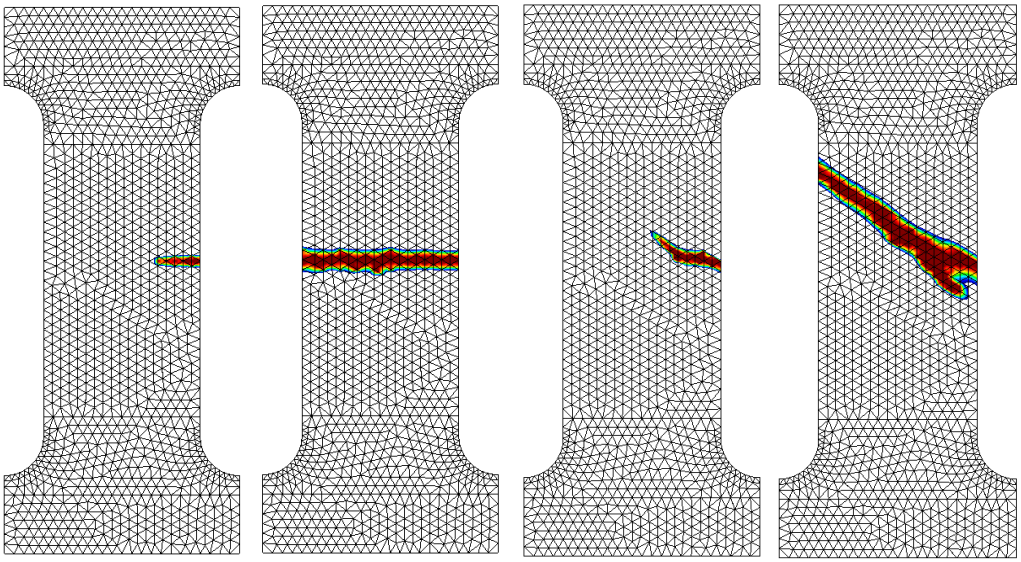

(a) Both cases, step = 0. (b) Isotropic case, step = 201. (c) $m = 45^o$, step = 178. (d) $m = 45^o$, step = 201.

Figure 1 – (a) Initial horizontal damage of 0.99 imposed on nodes (b) Final damage distribution and crack path for the isotropic case (c-d) Damage distribution and crack path for the anisotropic case.

From Figure 1(c), it can be seen that, for $\beta = 10$, the material behaves anisotropically, since the damage increased predominantly in the direction -45^0. And as expected, by setting $\beta = 0$, the material has an isotropic behavior and the crack remains at 0^0.

A second example is a single notched tensile test of a squared plate of dimensions $1m \times 1m$ with a horizontal notch in the middle of the plate height with half width length and preferential direction oriented at -45^o. For this simulation, a mesh of triangular linear elements and 3325 nodes was used (Fig. 2(a)). The plate is constrained at its botton edge while a prescribed displacement of $1 \times 10^{-4} tm/s$ is applied to the top edge. In this simulation, the following parameters are used $E = 200GPa$, $\nu = 0.3$, $\rho_0 = 7800 kg/m^3$, $l = 2.5 \times 10^{-3}$, $\tilde{b} = 1$ and $g_c = 2.7 \times 10^3 Nm$. The parameter β was fist assumed zero to recover the isotropic case and than for the anisotropic case two values were considered, $\beta = 10$ and $\beta = 20$.

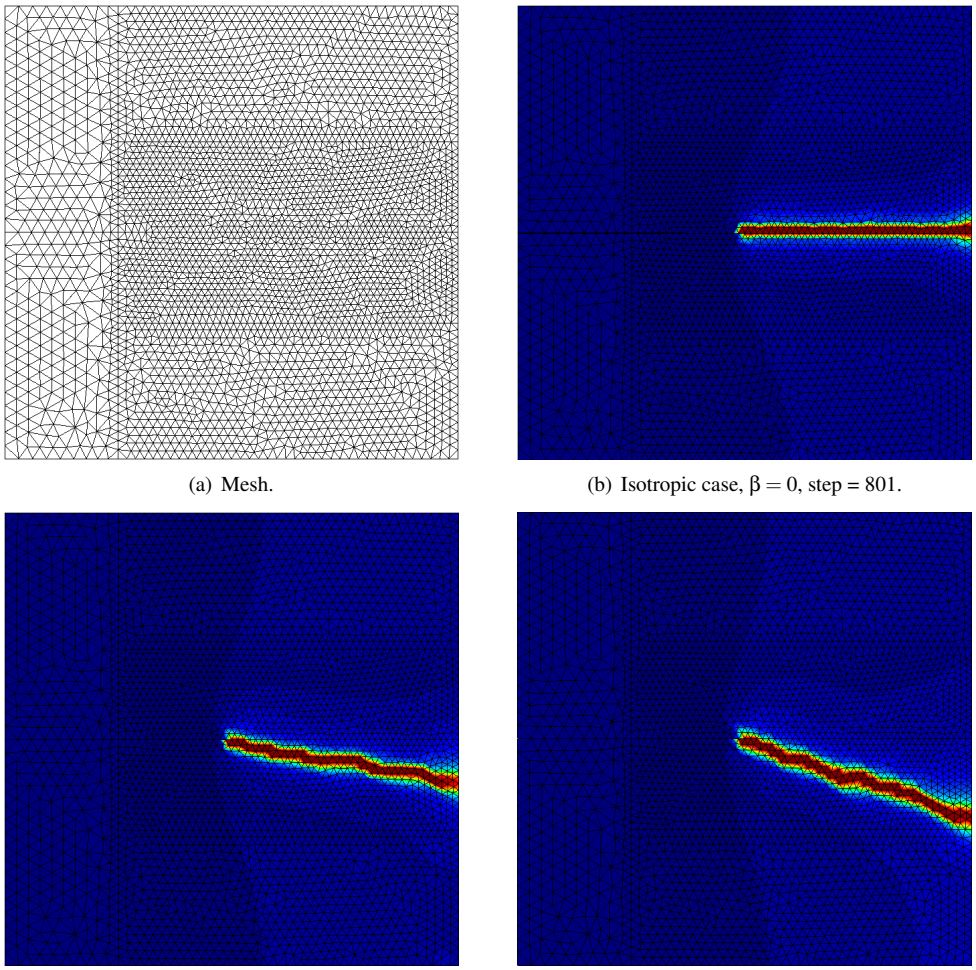

(a) Mesh.

(b) Isotropic case, $\beta = 0$, step = 801.

(c) $m = 45^o$, $\beta = 10$, step = 862.

(d) $m = 45^o$, $\beta = 20$, step = 934.

Figure 2 – (a) Mesh used for the single notched tensile test (b) Final damage distribution for the isotropic case (c-d) Damage distribution for the anisotropic case.

Figure 2(c) shows that for $\beta = 10$, there is a smaller angle between the direction of crack propagation and the horizontal direction. For $\beta = 20$ (Fig. 2(d)), the crack propagation angle also increases, tending to be closer to the material preferential direction of damage (-45^o). For a smoother crack path, it is necessary to increase the number of elements in the region of possible crack propagation.

Conclusion

The results showed that the model was capable to recover the isotropic damage evolution. It was also able to reproduce the expected crack propagation pattern for a material with initial damage at 0^0 and preferential cleavage plane oriented at -45^o. The effect of the parameter β, that regulates how strong is the fracture anisotropy, could also be observed for a notched tensile test example. Future analyses will include the effect of more than one preferential direction and also temperature and fatigue.

REFERENCES

Boldrini, J. L., Barros de Moraes, E. A., Chiarelli, L. R., Fumes, F. G., and Bittencourt, M. L. (2016). A non-isothermal thermodynamically consistent phase field framework for structural damage and fatigue. *Computer Methods in Applied Mechanics and Engineering*, 312:395–427.

Borden, M. J., Verhoosel, C. V., Scott, M. A., Hughes, T. J., and Landis, C. M. (2012). A phase-field description of dynamic brittle fracture. *Computer Methods in Applied Mechanics and Engineering*, 217-220:77 – 95.

Cahn, J. W. (1959). Free energy of a nonuniform system. II. Thermodynamic basis. *The Journal of Chemical Physics*, 30(5):1121–1124.

Chiarelli, L. R., Fumes, F. G., de Moraes, E. A., Haveroth, G. A., Boldrini, J. L., and Bittencourt, M. L. (2017). Comparison of high order finite element and discontinuous Galerkin methods for phase field equations: Application to structural damage. *Computers and Mathematics with Applications*, 74(7):1542–1564.

Clayton, J. D. and Knap, J. (2015). Phase field modeling of directional fracture in anisotropic polycrystals. *Computational Materials Science*, 98:158–169.

Miehe, C., Hofacker, M., and Welschinger, F. (2010). A phase field model for rate-independent crack propagation: Robust algorithmic implementation based on operator splits. *Computer Methods in Applied Mechanics and Engineering*, 199(45-48):2765–2778.

Mozaffari, N. and Voyiadjis, G. Z. (2015). Phase field based nonlocal anisotropic damage mechanics model. *Physica D: Nonlinear Phenomena*, 308:11–25.

Nguyen, T. T., Réthoré, J., and Baietto, M.-C. (2017). Phase field modelling of anisotropic crack propagation. *European Journal of Mechanics - A/Solids*, 65:279–288.

Teichtmeister, S. and Miehe, C. (2015). Phase-Field Modeling of Fracture in Anisotropic Media. *PAMM*, 15(1):159–160.

RESPONSIBILITY NOTICE

The authors are the only responsible for the printed material included in this paper.